ELSEVIER

Materials Characterization 54 (2005) 141–147

MATERIALS CHARACTERIZATION

Effect of texture on corrosion behavior of AISI 304L stainless steel

B. Ravi Kumar[a,*], Raghuvir Singh[a], Bhupeshwar Mahato[a], P.K. De[a], N.R. Bandyopadhyay[b], D.K. Bhattacharya[a]

[a]*National Metallurgical Laboratory, Jamshedpur, 831007 Jharkhand, India*
[b]*Bengal Engineering College, Howrah, India*

Received 12 March 2004; received in revised form 19 July 2004; accepted 30 September 2004

Abstract

Electrochemical behavior of austenitic AISI 304 stainless steel in two different solutions is presented here. Effect of cold rolling conditions on corrosion behavior of the steel is studied with respect to strain-induced α′-martensite phase, residual stress, and texture of both the austenite and α′-martensite phases. The annealed steel plate has been unidirectionally cold, rolled-up to 90% reductions. X-ray diffraction (XRD) technique has been employed to quantify the volume fractions of austenite and martensite phases and to study the textural development in the steel in rolled conditions. The presence of close pack crystallographic planes parallel to the specimen surface found to improve the corrosion properties.

Keywords: Austenitic steel; Cold rolling; Texture; Corrosion

1. Introduction

Austenitic stainless steels (SS) are good corrosion-resistance alloy steels. These steels mainly find their use in aggressive environments. AISI 304 SS, general-purpose steel, are widely used in the industry for applications related to corrosion-resistance. Corrosion resistance of these steels depends on various metallurgical variables [1]. AISI 304 SS becomes microstructurally unstable at room temperature when deformed and transformed to α′-martensite phase [2–6]. The presence of α′-martensite phase deteriorates the corrosion-resistance of the steel by selective anodic dissolution. In addition to strain-induced phase transformation during cold rolling, it develops very strong preferred crystallographic orientation in the parent austenite phase and the product α′-martensite phase. In the present investigation, an effort has been made to study the effect of α′-martensite volume fraction, residual stress (RS), and texture on the electrochemical behavior of 304 SS.

2. Experimental

AISI 304L SS grade steel plate of 10 mm thickness was solution-treated at 1080 °C for 1 h and quenched

* Corresponding author. Tel.: +91 657 2271709; fax: +91 657 2270527.
E-mail address: ravik@nmlindia.org (B. Ravi Kumar).

1044-5803/$ - see front matter © 2004 Elsevier Inc. All rights reserved.
doi:10.1016/j.matchar.2004.11.004

Table 1
Chemical composition of the 304L stainless steel

Elements	C	Si	Mn	P	S	Cr	Ni	N
Wt.%	0.03	0.54	1.8	0.028	0.014	18.55	9.5	0.04

in water to achieve chemical homogeneity. Table 1 shows the chemistry of the of the steel. Samples of 15×3 cm size were cut for cold rolling. These were cold rolled to 10%, 30%, 50%, 70%, and 90% of thickness reduction. The volume percent of strain induced α′-martensite phase formed by cold rolling was determined by X-ray diffraction (XRD) technique. Texture measurements were made on rolling plane by Schultz reflection technique [7] on 3×3 cm size specimens cut from the rolled sheet material. Pole figures of (111), (200), and (220) planes for austenite phase and (110), (200), and (211) planes for martensite phase were recorded. The Seifert XRD 3003PTS with Co Kα radiation was used for all XRD studies. The experimental pole figure data were used to calculate orientation distribution function (ODF) plots. RS measurements were carried out on all the cold rolled samples using XRD by $Sin^2\Psi$ method.

The anodic polarization measurements were performed on rolling plane in 1 N sulfuric acid (H_2SO_4) as well as in 0.1 N sodium chloride (NaCl) solutions. The solutions were prepared by adding the requisite amount of AR grade chemicals to the distilled water. The specimens of the size 10×10 mm were mounted on the araldite to expose 1 cm^2 area to the experimental solution. Samples for polarization study were polished up to 1200 grit emery papers followed by degreasing in acetone solutions before mounting on to araldite. The rear surface of the specimen was connected through a copper wire to the potentiostat; copper wire was insulated to isolate it from the solution. Before polarizing, the specimens were cathodically cleaned at a potential of −900 mV with respect to Saturated Calomel Electrode (SCE) for 120 s to remove the preexisting oxides, if any. Scanning was initiated at a potential of −100 mV with respect to the open circuit potential (OCP) at a scan rate of 6 V/h. It was then reversed (in NaCl solutions) after the current reached 0.5 mA in the transpassive region. The specimens, after anodic polarization tests, were examined under the optical microscope to ensure that no crevice formation occurs at the interface of araldite and working electrode. The saturated Calomel electrode was used as a reference electrode. The PARC 273 model Potentiostat/Galvanostat equipped with corrosion software was used for conducting electrochemical polarization experiments.

3. Results and discussion

3.1. Texture in austenite phase

The (111) pole figures of austenite phase at various rolling reduction levels are shown in Fig. 1. Main texture component of the austenite phase forms even at around 30% cold reduction in thickness. The pole figures of the rolled sheets suggest that initial rotation after small rolling reduction levels are towards orientation of the type {011}<100>. After heavier reductions brass type texture, a strong texture component corresponding to ideal orientation {011}<211> is apparent. The orientation distribution function analysis has revealed the presence of texture components {011}<100> G (gauss), {011}<211> Bs

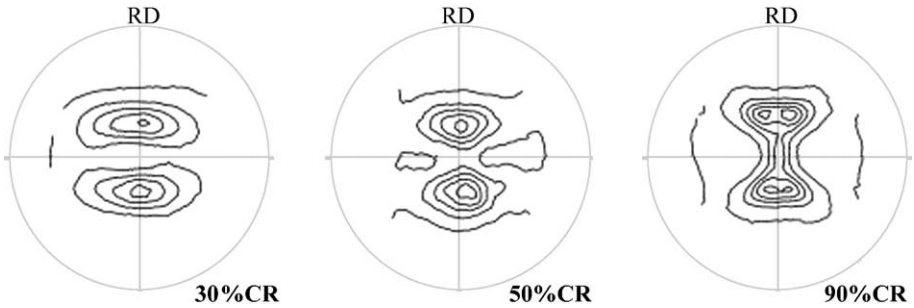

Fig. 1. {111} pole figures of austenite phase of specimens at different thickness reductions.

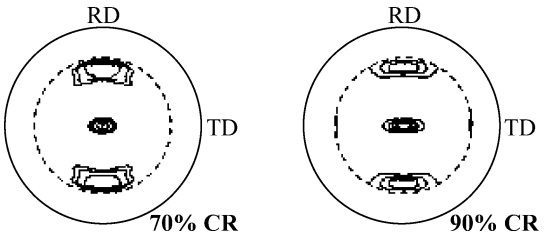

Fig. 2. {211} pole figures of martensite phase of specimens at different cold reduction thickness.

(brass), {011}<211> S, and {112}<111> C (copper) up to 70% cold reduction and above this, {112}<111> C disappears with the increase in the {011}<211> Bs orientation. Under all situations, the {011} planes, which are of medium close-packed planes, is the dominating orientation parallel to the specimen surface.

3.2. Texture in strain-induced martensite phase

The (211) pole figures of martensite phase at different cold reductions in thickness are shown in Fig. 2. The intensity of the poles increases with increasing cold reduction. The main texture components, {111}<112>, {112}<110>, and {001}<110>, with increasing intensities are obtained from the ODF analysis (Fig. 3). Therefore, formation of α'−martensite leads to development of crystallographic texture having close-packed {111}, {112}, and {001} planes parallel to the specimen surface.

3.3. Residual stress and strain induced martensite

XRD quantitative phase analysis results of the cold rolled samples are shown in Table 2. The volume

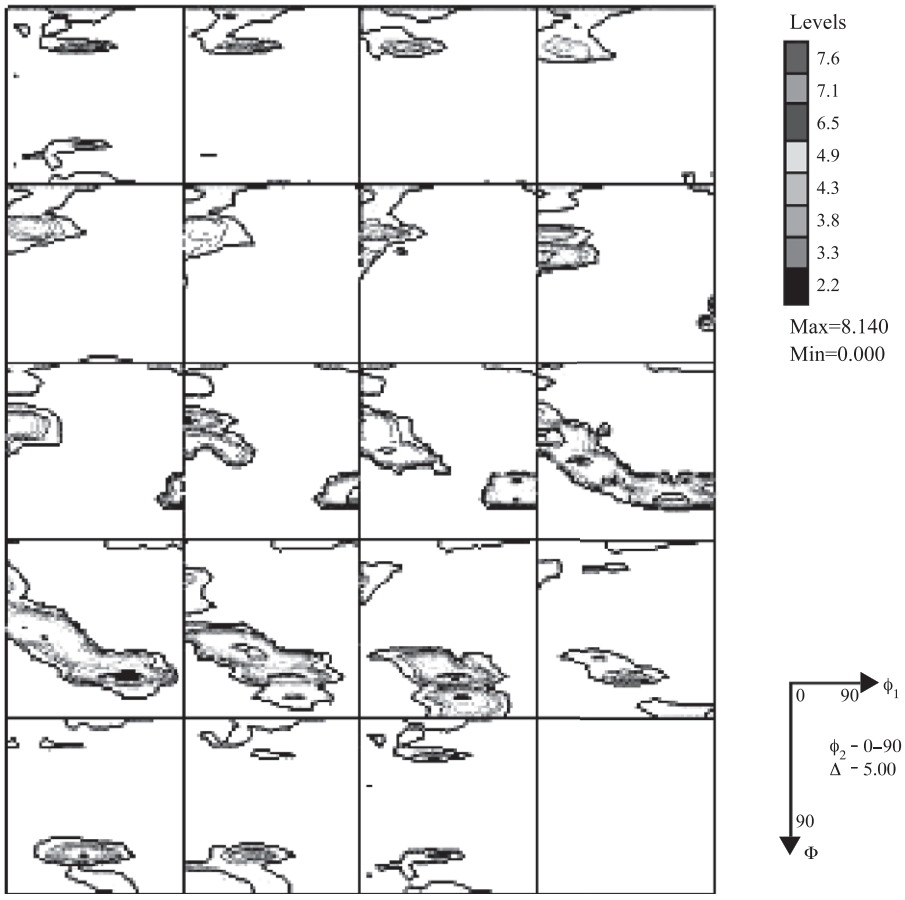

Fig. 3. ODF of martensite phase of 90% cold rolled specimen.

Table 2
Volume fraction of martensite phase during different cold rolling reductions

% CR reduction	Volume fraction of martensite phase
30	8
50	12
70	13
90	25

fraction of strain induced α′-martensite phase in the specimens found to increase with the percent cold reduction. RS in both the phases are shown in Table 3. As expected, RS is found to decrease in austenite phase due to strain-induced transformation and increase in α′-martensite phases due to continuous strain hardening with increasing cold reduction.

3.4. Electrochemical behavior of the steel

The electrochemical polarization curves of deformed as well as of solution-treated AISI 304L SS showed active–passive behavior in H_2SO_4 solutions; however, in NaCl solution, active region did not appear and steel remained passive even at an open circuit potential, as apparent from Figs. 4 and 5. The polarization curves of specimens in H_2SO_4 solutions, shown in Fig. 4, delineate changes that occurred during the passivation and prepassive regions. The higher currents of cold rolled up to 50%, than the base material, during passivation in H_2SO_4 solution indicates the effect of cold deformation parameters on the oxide film behavior [8,9]. This could be due to rolling residual tensile stresses generated in the system or formation of α′-martensite. The low deformation was found to increase the passivation current, and further increase in deformation reduces it. Development of sharp crystallographic texture in austenite as well as α′-martensite phase occurs at high-cold reduction levels compared to

Table 3
Residual stresses developed during different cold rolling reductions

% CR reduction	Residual stress in MPa	
	Austenite	α′-martensite
30	134	–
50	151	12
70	141	13
90	136	24

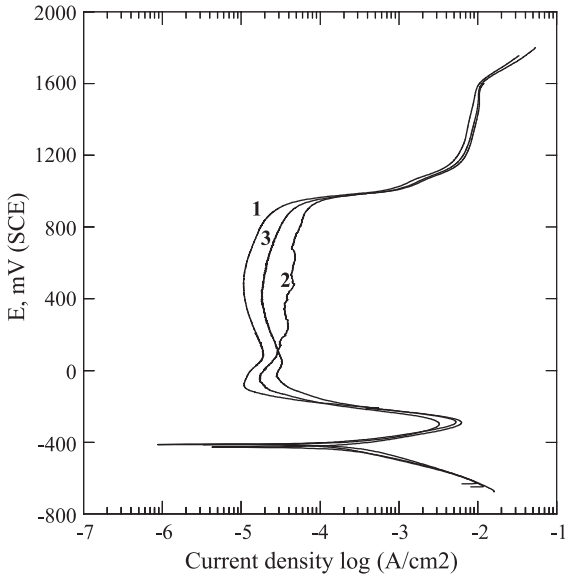

Fig. 4. Electrochemical polarisation curves of (1) base samples, (2) 30% cold rolled, and (3) 90% cold rolled in H_2SO_4 solution.

at low deformation. Both the phases have shown the rolling plane crystallographic texture of {110} in austenite and {111}, {112}, and {001} in α′-martensite phases. It is reported that high-density close-packed crystal planes offer better resistance to chemical attack and better passivation and repassivation characteristics

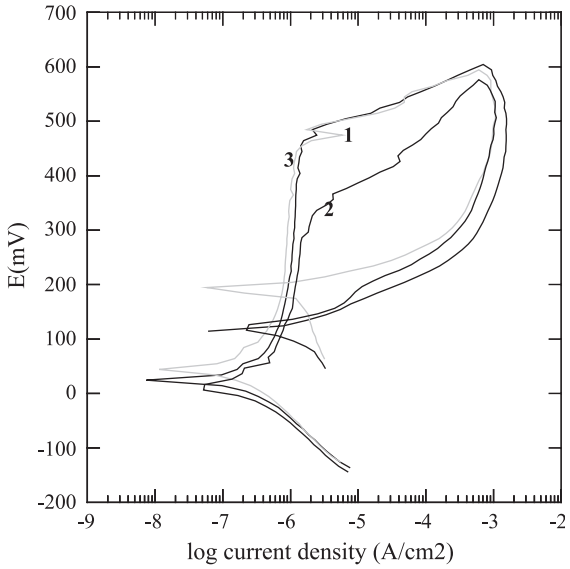

Fig. 5. Electrochemical polarisation curves of (1) base samples, (2) 30% cold rolled, and (3) 90% cold rolled in NaCl solution.

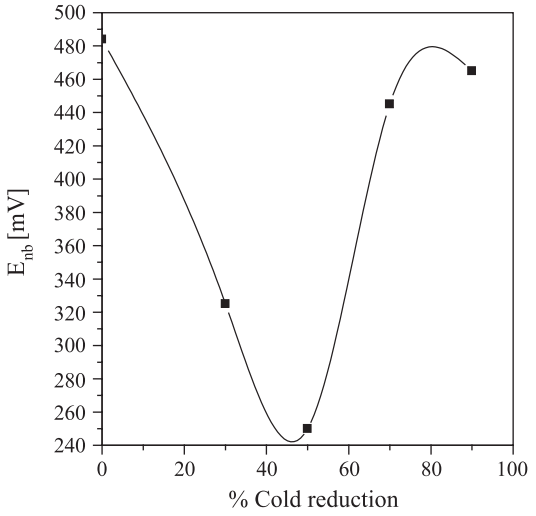

Fig. 6. Variation of pitting potential with % cold reduction in NaCl solution.

[10]. In the present study, austenite (f.c.c.) and α′-martensite (b.c.c.) phases offer high-packing density crystal faces of type {110} of f.c.c. and {111}as well as {001} of b.c.c. to the solution attack. The effect of rolling tensile residual stress, which has an adverse effect on passivation and prepassivation characteristics, appears to be nullified by the beneficial crystallographic orientation at higher reductions. Hence, at higher deformation, the crystallographic orientation developed in the specimen improves passivation and prepassivation characteristics. On annealing 90% cold rolled specimen up to 400 °C, polarization curves did not depict the change in the passive current as well as in primary passive current. However, annealing up to 400 °C found to decrease the residual stress without having any effect on texture and volume fraction of α′-martensite. This observation therefore supports our conclusion that, at lower reduction, passivation and repassivation characteristics are governed by rolling tensile stresses, and at higher reductions, it is taken over by texture in the material. This shows that residual stress does not play an important role in altering the corrosion kinetics during passivation in sulfuric acid solutions at higher reductions. The role of cold rolling and stresses in earlier studies has shown quite controversial, i.e., including insignificant changes besides reducing or decreasing affects on passivation [8,11]. The effects would be prominent when rolling does bring about the compositional changes in austenite and α′-martensite phases in the material.

The pitting potential, E_{nb}, of various cold rolled stainless steel samples determined in 0.1 N NaCl solutions is plotted against % cold deformation in Figs. 6 and 7. The pitting susceptibility was observed to vary with % cold rolling. The variation in pitting potentials, in NaCl solution, with increase in cold ,work has also been mentioned by several researchers [12–16]. However, the nature and extent of variations are widely scattered [12–16], probably due to the difference in method of evaluation, e.g., scratch tests [12,14], anodic polarization [12,13,15,16], PPR [13], experimental parameters, e.g., solutions, temperature, pH, etc. [15,16], or the extent of deformations. A large shift in pitting potentials of deformed steels may be seen when chloride content is increased similar to the deformation [17]. The changes in pitting potential, in cold deformed steel or iron, have been reportedly attributable to stress, deformation-induced α′-martensite, or dislocations. In our results, the cold reduction up to 50% was found to reduce the pitting potential while it increases the E_{nb} of base steel beyond 50%. Similar behavior has been shown by earlier reports after deformation up to 50% [12,14,16]; however, a few have shown it to be opposite [13,15]. The role of α′-martensite has been contradictorily reported with

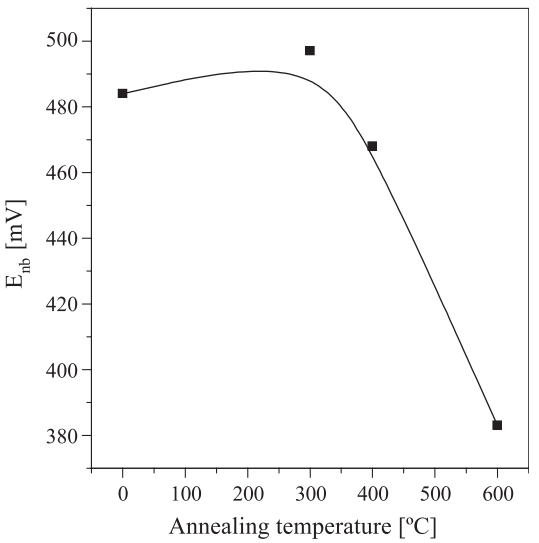

Fig. 7. Variation in pitting potential of 90% cold rolled sample after annealing treatment in NaCl solution.

regard to changes, e.g., increase, decrease, or insignificant in the pitting potential [12–14,18,19]. One possible reason may be the restricted deformation applied (max 50%) up to which the pitting susceptibility showed a monotonous change and therefore could be related to increasing % α′-martensite (as α′-martensite in 304L SS increases with % cold work). In the present study, the stainless steels was deformed to a much higher level, e.g., 90% during which pitting potentials was found to be varied in a sinusoidal manner. The variation in pitting potential does not appear to have a direct correlation with increase in the % α′-martensite, as a result of cold deformation from 0–90% (comparing Fig. 6 and Table 2), and therefore, the effect of α′-martensite may not be expected to cause change in E_{nb}. The insignificant effect of cold deformation and deformation-induced α′-martensite on pitting potential has already been demonstrated by a few of earlier reports [12–14,18–20], although pit density was shown to be increased with deformation. The change in the pitting potential of SS 304L in the present study may, rather, be explained due to the effect of stresses, crystallographic texture, or combination thereof. The decrease in pitting potential at low (<50%) deformation is possibly due to high residual tensile stresses, as it is being known to be detrimental for corrosion resistance [1]. The effect of texture at low deformations (<50%) may be insignificant due to their low intensity. However, it becomes more prominent at higher deformations, and tensile stress decreases. It has been demonstrated earlier that, in Fe–Cr alloys, a major textural component play a role to enhance Cr diffusion [21]. Moreover, recent study showed that the passive film formed on highly deformed (~66%) SS 304L contains higher Cr/Fe ratio than that in the film on annealed one and attributable to higher pitting potential than the later [22]. Similar changes in the diffusion of Cr during passivation after cold deformation have also been indicated earlier [17,23]. Stainless steel cold-worked beyond 50% has high-density close-packed planes, which seems to have favored the formation of Cr-rich passive film that enhances the pitting potential. In addition, tensile stresses tend to decrease at higher deformation which is beneficial and that may have added to pitting resistance. However, annealing the 90% rolled specimen up to 300 °C does not effect the pitting resistance (Fig. 7). Above 300 °C, it begins to deteriorate, which is unexpected, as there is no changes in terms of phases or texture was observed. This is unlike our observation in sulfuric acid solution that showed dependence to crystallographic texture of the material in annealing condition too.

The above observations indicate that the presence of high-density close-packed crystallographic faces of specimen parallel to the surface nullifies the adverse effect of the tensile residual stress in controlling the pitting behavior of the SS 304L. The results have shown that annealing up to 500 °C temperature, texture, and martensite did not change while stresses and dislocation density as a result of recovery of deformed structure are significantly reduced. Despite these favorable changes, the susceptibility of steel to pitting corrosion is found to increase above 300 °C. Crystallographic texture seems to play an important role to alter pitting mechanism, possibly by reducing favorable sites for corrosion attack and formation of Cr-rich passive film favored by high-density close-packed planes oriented to the rolling surface. The one to one correlation of individual metallurgical changes, i.e., texture, stresses, α′-martensite, and dislocation density, with corrosion resistance is made possible by sequential removal of stress and second phase by annealing treatment.

4. Conclusions

Electrochemical and pitting potential behavior of the cold rolled AISI 304L stainless steel in sulfuric acid and sodium chloride solution is found to be controlled by tensile rolling stresses at lower cold reduction levels where cold rolling texture begins to develop. At large deformations, sharp rolling texture of the AISI 304L SS seems to nullify the adverse effect of the cold rolling residual stresses. The strain induced α′-martensite although expected to deteriorate the corrosion properties in the presence of tensile stress; however, in the present study, the texture of the material is found to minimise it.

Acknowledgments

The authors are grateful to Professor S.P. Mehrotra, Director, National Metallurgical Laboratory, for supporting this work and for the permission to publish.

References

[1] Hanninen HE. Influence of metallurgical variables on environment-sensitive cracking of austenitic alloys. Int Mater Rev 1979;3:85–135.

[2] Manganon Jr PL, Thomas G. The martensite phases in 304 stainless steel. Metall Trans 1970;1:1577–86.

[3] Manganon Jr PL, Thomas G. Structure and properties of thermal-mechanically treated 304 stainless steel. Metall Trans 1970;1:1587–94.

[4] Hecker SS, Stout MG, Staudhammer KP, Smith JL. Effect of strain state and strain rate on deformation induced transformation in 304 stainless steel: magnetic measurements and mechanical behavior. Metall Trans 1982;13A:619–26.

[5] Olson GB, Cohen M. Kinetics of strain-induced martensitic nucleation. Metall Trans 1975;6A:791–5.

[6] Maxwell PC, Goldberg A, Shyne JC. Stress-assisted and strain-induced martensites in FE–NI–C alloys. Metall Trans 1974;5:1305–24.

[7] Schulz LG. Schultz reflection method. J Appl Phys 1949;20:1030–3.

[8] Foroulis ZA, Uhlig HH. Effect of cold-work on corrosion of iron and steel in hydrochloric acid. J Electrochem Soc 1964;111:522–8.

[9] Barbucci A, Delucchi M, Panizza M, Sacco M, Cerisola G. Electrochemical and corrosion behaviour of cold rolled AISI 301 in 1 M H_2SO_4. J Alloys Compd 2001;317–318:607–11.

[10] Chouthai SS, Elayaperumal K. Texture dependence of corrosion of mild steel after cold rolling. J Brit Corros 1976;11:40–3.

[11] Evans UR. Corrosion and oxidation of metals. London: Edward Arnold; 1960. p. 386.

[12] Maza B, Pedeferri P, Sinigaglia D, Cigada A, Mondora GA, Re G, et al. Pitting resistance of cold worked commercial austenitic stainless steels in solutions simulating to seawater. J Electrochem Soc 1979;126:2075–81.

[13] Syrett BC, Wing SS. Pitting resistance of new and conventional orthopedic implant materials–effect of metallurgical condition. Corrosion 1978;34:138–45.

[14] Semino CJ, Pedeferri P, Burstein G, Hoar TP. The localized corrosion of resistant alloys in chloride solutions. Corros Sci 1979;19:1069–78.

[15] Mudali UK, Shankar P, Ningshen S, Dayal RK, Khatak HS, Baldev Raj. On the pitting corrosion resistance of nitrogen alloyed cold worked austenitic stainless steels. Corros Sci 2002;44:2183–98.

[16] Mudali UK, Ningshen S, Tyagi AK, Dayal RK. Influence of metallurgical and chemical variables on the pitting corrosion behaviour of nitrogen-bearing austenitic stainless steels. Mat Sci Forum 1999;318–320:495–502.

[17] Barbucci A, Cerisola G, Carbot PL. Effect of cold working in the passive behavior of 304 stainless steels in sulfate media. J Electrochem Soc 2002;149:B534–42.

[18] Cigada A, Rondelli G, Vicentini B. Proc. Int. Conf. Martensitic Transformation, Sendai, Japan: The Japan Institute of Metals; 1986. p. 527–32.

[19] Eckstein Ch, Welss A, Janke D, Peisker D. Proc. Int. Cong. Stainless steels 99, Science and Market, Chia Laguna Sardinia, Italy, 1999. Italy: Associaziona Italiana di Metallurgia; 1999 (June 6–9). p. 34–42.

[20] Randak A, Trautes FW. Influence of austenite stability of 18–8 chromium–nickel steels on their cold working and corrosion properties. Werks Korros 1970;21:97–109.

[21] McBee CL, Krugher J. Nature of passive films on iron–chromium alloys. Electrochim Acta 1972;17:1337–41.

[22] Phadnis SV, Satpati AK, Muthe KP, Vyas JC, Sundareshan JC. Comparison of rolled and heat treated SS304 in chloride solution using electrochemical and XPS techniques. Corros Sci 2003;45:2467–83.

[23] Singh R, Ravi Kumar B, Kumar A, Dey PK, Chattoraj I. The effects of cold working on sensitization and intergranular corrosion behavior of AISI 304 stainless steel. Metall Trans 2003;34A:2148–441.